

IAC-10.B2.4.8

AN EXTENSIVE AND AUTONOMOUS DEEP SPACE NAVIGATION SYSTEM USING RADIO PULSARS

A.A.Kestilä

Aalto University, School of Science and Technology, Finland, akestila@cc.hut.fi

S. Engelen

Delft University of Technology, Faculty of Aerospace Engineering, Chair of Space Systems Engineering, The Netherlands, s.engelen@tudelft.nl

E.K.A. Gill

Delft University of Technology, Faculty of Aerospace Engineering, Chair of Space Systems Engineering, The Netherlands, E.K.A.Gill@tudelft.nl

C.J.M. Verhoeven

Delft University of Technology, DIMES, The Netherlands, C.J.M.Verhoeven@tudelft.nl

Prof. Dr. M.J. Bentum

University of Twente, Faculty of EEMCS, Short Wave Radio Chair, The Netherlands, M.J.Bentum@ewi.utwente.nl

Z. Irahauten, PhD

Delft University of Technology, Faculty of EEMCS, Wireless and Mobile Communications Group (WMC), The Netherlands, Z.Irahauten@tudelft.nl

Interstellar navigation poses significant challenges in all aspects of a spacecraft. One of them is reliable, low-cost, real-time navigation, especially when there is a considerable distance between Earth and the spacecraft in question. In this paper, a complete system for navigation using pulsar radio emissions is described and analysed.

The system uses a pulsar's emissions in the radio spectrum to create a novel system capable of fully autonomous navigation. The system is roughly divided into two parts, the front - end and the back - end, as well as their subdivisions. The front - end performs initial signal reception and pre-processing. It applies time-based coherent de-dispersion to allow for low-power on-board processing, and uses a very wide bandwidth to limit the required antenna size. As a result, the electronics required performing the processing is complex, but the system is well limited in both size and power consumption.

The back-end, in turn, performs advanced nonlinear Kalman filtering and supplies the final navigational product - the systems complete (position and velocity) state vector, as well as the involved uncertainties. Rather uniquely, it uses two inherent signal properties, the Doppler shift and the inherent pulse period slowdown, simultaneously, to obtain both a relative and an absolute estimate of the spacecraft's position. Combined, in the nonlinear Kalman filter, they result in the complete state vector of the system.

Performance of the system was analysed and validated using actual telescope data from the LOFAR array.

The results show that the front-end can indeed receive and process even a very weak signal from an actual pulsar, while the back-end can output a navigational product despite significant random noise in the signal data received from the front-end.

INTRODUCTION

Pulsars are extremely stable timing sources, and spread widely throughout the galaxy, with a modest bias towards the galactic core. These properties, combined with their known angular positions in a celestial frame of reference, make them ideal navigating beacons. Such a navigation principle however has never been thoroughly tested, hence a proof-of principle was deemed in order.

The authors prepared a simulation of a generic pulsar navigation system, of which an overview is shown in Fig. 1. The received signals are fed to the

front-end signal processing, which takes care of folding and de-dispersing the signals, and provides time-of arrival estimation to the back-end, which in turn uses the information to extract the relative velocities to each received pulsar. These velocities, combined with their known angular positions is then used as an input to an unscented Kalman filter, which updates the receiver's state-vector at equal update intervals.

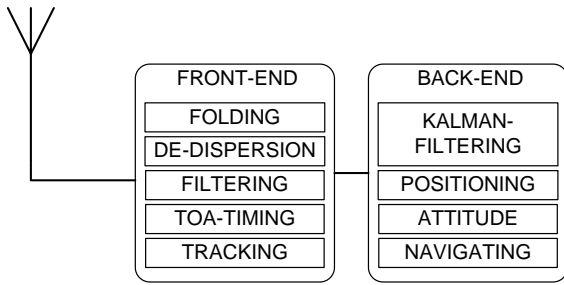


Fig. 1: The principle of the envisaged pulsar-based navigation system

The main problem areas immediately identifiable are in actually receiving the pulsar signals, in accurately extracting the timing information, and in developing a Kalman filter that would be suitable to the problem at hand.

The system was divided into two distinct subsystems: a front-end and a back-end. (cf. Fig. 2) Each subsystem was simulated and the simulations were verified using actual telescope data.

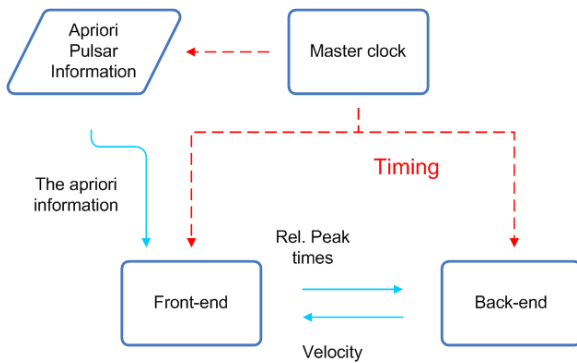


Fig. 2: System interfacing

THE FRONT END

The front end processes the data received through the antenna system. Baseband data is sampled, and consequently de-dispersed with the known dispersion properties of the pulsar. Subsequently, the data is folded at the pulsar's expected pulse period, in order to elevate the signal-to-noise ratio to useful levels. Folding at the expected pulse period will cancel out other signal sources in the data, which do not share similar pulse periods.

Matched filters finally confirm the location of the pulse profile in the data, after which the pulse arrival times are sent to the back-end.

Note the expected pulse periods are calculated for a given Doppler shift, and hence either a-priori velocity information is required, or a search will have to be performed at multiple Doppler shifts.

De-dispersion

Due to the Interstellar Medium (ISM), scattering and dispersion of the pulsar's signal occurs⁽¹⁾. This dispersion effectively forms a frequency dependent filter, causing a time delay in the arrival of the pulse at different frequencies.

Two well known methods combating this effect were used and simulated, and it was found that incoherent de-dispersion was much more robust against interference than coherent de-dispersion. Implementing an incoherent de-dispersion system in hardware however is a costly feature, which would severely limit the available signal bandwidth. A hybrid solution is therefore proposed, in which the channel bandwidth is determined by the pulsar with the largest dispersion measure. Within each channel, a coherent de-dispersion process is performed, after which the results of each individual channel are added to arrive at a high-bandwidth, de-dispersed signal.

The coherent de-dispersion algorithm used was given in Hankins and Rickett⁽²⁾. The transfer function was subsequently converted into the time-domain to increase the operating speed, as it was found the Fast Fourier Transforms (FFT) required for frequency-domain processing would greatly reduce the applicability of this system. All other filters used in the front-end were subsequently converted into the time domain as well, resulting in a massive increase in simulation and processing speed.

No loss in accuracy was observed.

Time of arrival estimation

Timing the pulse arrival times is quite cumbersome, as the de-dispersion and folding processes only work with any degree of accuracy once the exact receiver velocity with respect to the pulsar is known, due to Doppler shifts in the pulse and carrier frequencies. As this is the intended output of the system, a general search is used, assuming likely velocity candidates. The degree of accuracy of the determined velocity can be estimated through the drift time t_d , which is defined as the time it takes for a pulse peak position to drift out of a data bin.

As is shown in Fig. 3, the drift per period, relative to the pulse period, is equal to the difference in period length, dP . When considering each period P is divided into a given number of bins, n_{bins} , or samples, their time is definable as:

$$t_{bin} = \frac{P}{n_{bins}} \quad [1]$$

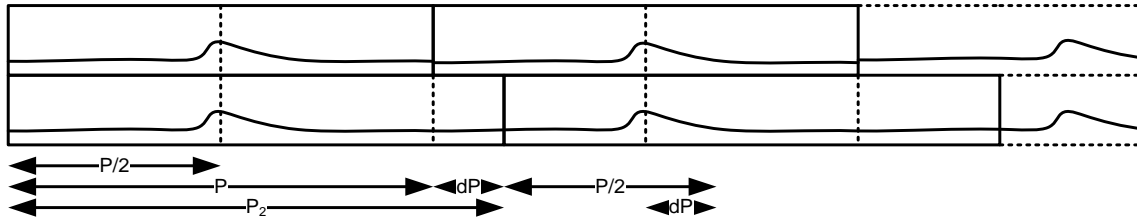


Fig. 3: Period definitions

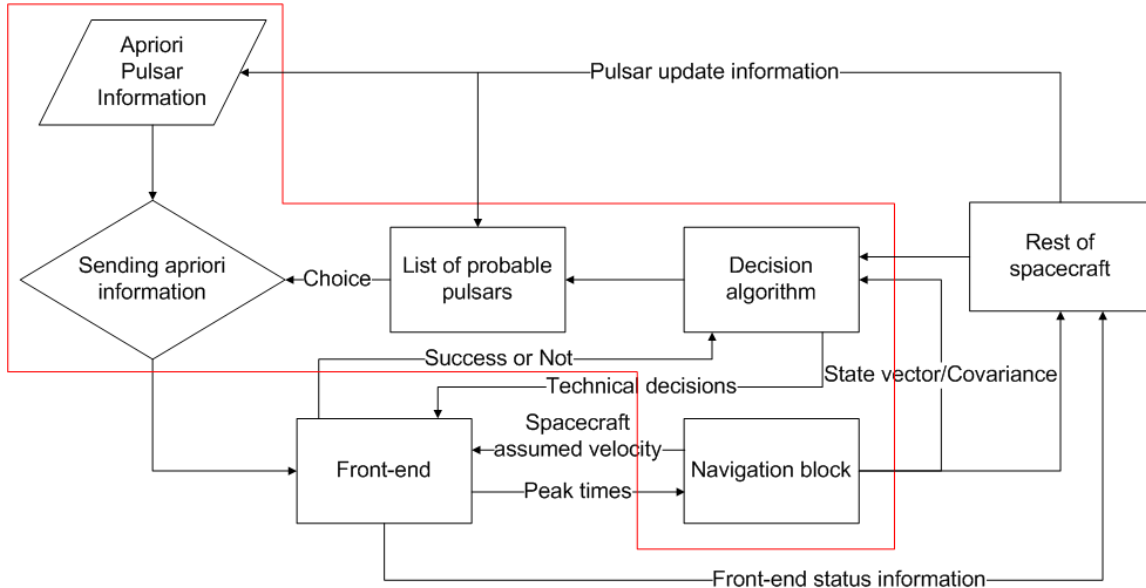


Fig. 4: The list-and-search approach functional flow.

This relation can be adapted to the change in bin time, equal to dP , according to:

$$t = \frac{P_2}{n_{bins}} \frac{P}{P_2 - P} \quad [2]$$

The original pulse period then equals:

$$P_{original} = n_{bin} \left(\frac{1}{t} + \frac{n_{bin}}{P_2} \right)^{-1} \quad [3]$$

This implies the only required variables to extract the correct folding-period are the number of bins taken per period, the period they were taken at and the time it takes for the pulse peak to shift by one single bin.

The more an assumed search velocity is off of the actual velocity, the faster the pulse will drift out of the initial peak bin, allowing for faster searches. With highly dispersed signals however, the de-dispersion process will cause the peaks to remain undetectable when the search velocity is off by

more than a few kilometers per second, limiting the search speed for such signals. Moreover, the signal-to-noise ratio will have to be sufficiently high, in

order for this method to work properly, as otherwise no pulses would be detectable in the data to apply this method on.

THE BACK-END

In the back-end, advanced filtering is performed on the relative peak times (instantaneous pulsar periods) coming from the front-end. Using these filtered peak times to perform navigation, through the use of two distinct methods. The end result is the full position and velocity state vector, as well as its associated covariance matrix. The main chosen frame of reference is at an independent location, such as J2000.0, and is separate from the spacecraft frame of reference, which is a non-orthogonal frame of reference, and transverse with respect to the pulsars themselves.

An important matter to point out is that any systematic error in the received pulsar signal can be modeled to sufficient accuracy and thus eliminated from it, such as relativistic effects, while the random noise can be taken care by the chosen advanced filtering method.

Front – end / Back-end interfacing

In practice, the front-end will be a black box to the back-end, with a desired output and a

controllable timing, navigational product velocity and a-priori information as inputs. The *a-priori* pulsar information consists of known pulsar properties, such as and most importantly, its period and period decay, as well as the pulsar's angular coordinates with respect to some chosen frame of reference.

Dependence on attitude

In order for the front-end to perform its task, it needs to know the attitude, and thus the field of view of its antenna receiver. This presents a problem, and has two solutions. The choice between these is about whether independent attitude information is available. If not, a separate and simple list-and-search function is required, with which the three minimum required pulsars can be found, see Fig. 4. However, this list-and-search approach, "blind man's attitude", works well only in the often exceptional situation, where the spacecraft possesses no angular velocity or acceleration with respect to the chosen main frame of reference. In the far more common case, the so-called "running blind man's attitude", where the spacecraft possesses angular velocity or acceleration, the situation becomes much more complicated and requires further studying. In this case, the list-and-search function has a time limit imposed on it, as the antenna field of view moves throughout the celestial sphere.

Navigation and attitude methods

Two specific navigational methods and a tentative attitude determination method were developed for the use of this pulsar navigation system. Both navigational methods stem from Time-Of-Arrival estimation⁽³⁾.

Doppler shift method

The received pulsar signal experiences a Doppler shift due to the spacecraft transverse velocity. By observing this Doppler shifted pulsar signal and comparing it with an 'ideal' transmitted pulsar signal, when the spacecraft is at rest with respect to some certain frame of reference, the Doppler shift can be compared with the first-order equation⁽⁴⁾,

$$\frac{P_0}{P_r} = \frac{1 - \frac{\bar{v} \cdot \bar{e}}{c}}{1 + \frac{\dot{P}}{P_0}(t - t_0)} \quad [4]$$

Where the subscript r denotes the value at the receiver, c is the speed of light, \bar{e} the unit attitude vector with respect to the chosen main frame of reference, P_0 initial period (a-priori known value) and t_0 initial time. For the sake of example, all

relativistic and potential effects have been neglected. This equation can be subsequently converted into the form

$$\left(1 - \frac{P_0}{P_r} \left(1 + \frac{\dot{P}}{P_0}(t - t_0) \right) \right) c = v \quad [5]$$

As \bar{e} is merely the direction of the pulsar, assumed to be along the non-orthogonal axis and so a unit vector, the instantaneous transverse velocity of the spacecraft is determined.

Pulse decay method

In order to find the spacecraft's instantaneous and absolute position with respect to a chosen frame of reference, the inherent pulsar property, the slow decay of the pulsar period, can be used. The main idea behind this method is the accurate modeling of the pulsar period and its decay, and their comparison with the received, true pulsar signal.

As a simple example, a one dimensional situation can be imagined. Here, the pulsar, the receiving spacecraft and a chosen main frame of reference are all in one line of sight. For a fairly accurate presentation of the pulsar signal, equation

$$P_{th} = P_0 + \dot{P}(t - t_0) \quad [6]$$

can be used⁽³⁾. If the spacecraft is indeed stationary with respect to the chosen frame of reference, the difference between the observed and theoretical (modeled) pulse periods, is

$$\Delta P = P_{obs} - P_{th} = \dot{P}\Delta t \quad [7]$$

Which can be rewritten as,

$$\Delta s = \frac{c \cdot \Delta P}{\dot{P}} \quad [8]$$

Here c is the speed of light, and Δs is the distance from the arbitrarily chosen frame of reference, pointing toward the pulsar, while N is random, Gaussian noise. The same can be done for a three dimensional situation, thus needing only a theoretical minimum of three pulsars.

Here, the assumption was that the spacecraft is stationary, which is a special case. Thus in reality, the kinetic effects on the received and modeled signals, manifests itself in the form of $\dot{P} = \dot{P}(\bar{r}, \bar{v}, \bar{a})$. This can be in turn modeled, when Equation 4 is differentiated with respect to time, giving

$$\frac{dP}{dt} = \frac{\frac{\dot{P}}{P_0} \left(1 - \frac{\bar{v} \cdot \bar{e}}{c}\right) - \left(1 + \frac{\dot{P}}{P_0} (t - t_0)\right) \left(\frac{-\bar{a}_r \cdot \bar{e}}{c}\right)}{\left(1 - \frac{\bar{v} \cdot \bar{e}}{c}\right)^2} \quad [9]$$

as the new \dot{P} to be used in Equations 7 and 8.

Advanced Filtering and integration

Within the back-end, advanced filtering is performed on the input peak times using an Unscented Kalman Filter (UKF). This filter can work with highly nonlinear force models to a more accurate degree, unlike the Linear Kalman Filter. In addition, Runge-Kutta-Nyström (RKN) is used as the numerical integration method for the spacecraft's orbit model and its propagation within the UKF.

Required ground segment

Pulsars are natural objects, and so can behave unpredictably. Two particular phenomena are of concern: Glitches and nullings.

A glitch is an apparent rapid change in the pulsar period and period decay, lasting from a few days up to months, and never regaining its original values⁽⁵⁾. A nulling, in turn, is simply the ceasing of emissions from the pulsar, causing the decay of the pulsar period to be shifted proportionally. Both of these require either adaptive methods on-board, in order to retain the use of the misbehaving pulsars, which likely means higher cost and complexity, or alternatively the spacecraft should rely on a limited ground segment. A so-called "weather station" could gather the periodical scans done by the radio astronomy community, and perform a general update broadcast after some certain amount of anomalies have occurred, so as to enable any listening spacecraft to update its *a-priori* information on all the disturbed pulsars.

So far, about 100 glitches in the past 30 years have been observed(1).

RESULTS

TOA accuracy is directly related to the bandwidth of the receiver, as the sample rate dictates the bin times. This limits the achievable velocity determining accuracy, and serves as an

error source of the input to the back-end. Moreover, false detections will occur in low SNR situations, or in case of improper filtering or de-dispersion. This is one of the primary reasons for setting up the simulation, and it should indicate which SNR ratios will be acceptable for such a system, for a given bandwidth. Eventually, the results should lead to an indication of the required antenna size.

Both an incoherent de-dispersion system and a coherent de-dispersion system were simulated, and their results can be compared, as is done in Table 1.

	Incoherent	Coherent
Bandwidth	521 Hz x 5 channels	1534 Hz
Acquisition time	200s	100s
Error for:		
SNR -10dB	0	0
SNR -15dB	0	3
SNR -45 dB	0	No match

Table 1: The simulation results for both systems. Errors are given in units of theoretically achievable velocity resolution

The results in Table 1 are in units of detection limits – the system is only able to distinguish between distinct velocity increments, due to the limited bandwidth. A value of 0 therefore implies the result was within the detection limits, whilst higher values are off by n times that particular limit. Note, these limits are quite severe, as the detection limit ranges from about 2.8 km/s for 500 Hz ($t_{int}=200s$), to 3.9 km/s for 1500 Hz ($t_{int}=100s$), due to the low bandwidth.

These results were obtained using plain folding methods, and a manual search routine, which is primarily the reason for the low amount of data-points. The results are quite clear – the coherent de-dispersion system is quite a lot less robust, and will therefore require a lot more filtering, or a more accurate algorithm.

Given the SNR ratios, and the related search times, large antennas and matched filters would be required to speed up the process and increase the sensitivity levels. In order for this system to be of any practical use, an increased bandwidth is highly recommended, as it lowers the velocity detection limit, and increases the signal strength quite dramatically.

VALIDATION

Front-end validation

The front-end was validated using data obtained from the LOFAR test antennas. The data was barycentered and phased to track B0329+54, but otherwise untouched.

B0329+54 is one of the strongest emitters amongst all known pulsars to date, and it has one of

the lowest dispersion measures, making it an ideal target to study.

The system was able to detect the pulsar, and calculate its transverse velocity as 91.77 km/s, which has a discrepancy of 6.45 km/s with respect to the 98.22 km/s provided by Lorimer et al.(6). Their data was sampled around 1995 however, whilst ours was taken in 2009 and our data had a limited bandwidth of approximately 770 Hz, which gives the system a velocity resolution of +/- 780 m/s after 500 s of integration, which could both allow for some of the discrepancy.

More pulsars were found in the data, yet determining their transverse velocities was not possible due to the long search times involved. The pulsars found were B0320+39, B0450+55, B0355+54 and B0353+52, all of which are within a narrow cone around the central target pulsar.

Back-end validation

In addition, the functioning of the back-end and especially the advanced filtering used was validated.

A simplified trial case of the Earth circling the Sun was applied, and a severely noisy pulsar signal was generated for the task. Earth itself was

considered to be the receiver. This noisy signal was then modified to be received as if the signal came from three different pulsars, all situated infinity away on the axis' of an inertial J2000.0 frame of reference.

In order to make sure the UKF worked as intended, back-up validation was done with Least-Squares Estimation. As case-examples, for a ten day period and a sample time of 100 seconds, Fig. 5 and Fig. 6 show the orbit is clearly revealed from the enormous amount of noise imposed on the pulsar signal. The random noise had a standard deviation, σ of 31 meters.

Fig. 5 shows the difference between the 'true' total orbital state vector (x, y and z position components, as well as v_x , v_y and v_z velocity components) and that generated by the UKF based on the received pulsar signals. As can be seen, the difference is very small, while the wobble seen in most of the component plots is due most likely to unrelated computational errors. Fig. 6 in turn shows the UKF's measurement residual plot for the position state vector, and it can be seen that the imposed random noise on the pulsar signal shows up in here as well, meaning the UKF has successfully extracted it from the final result.

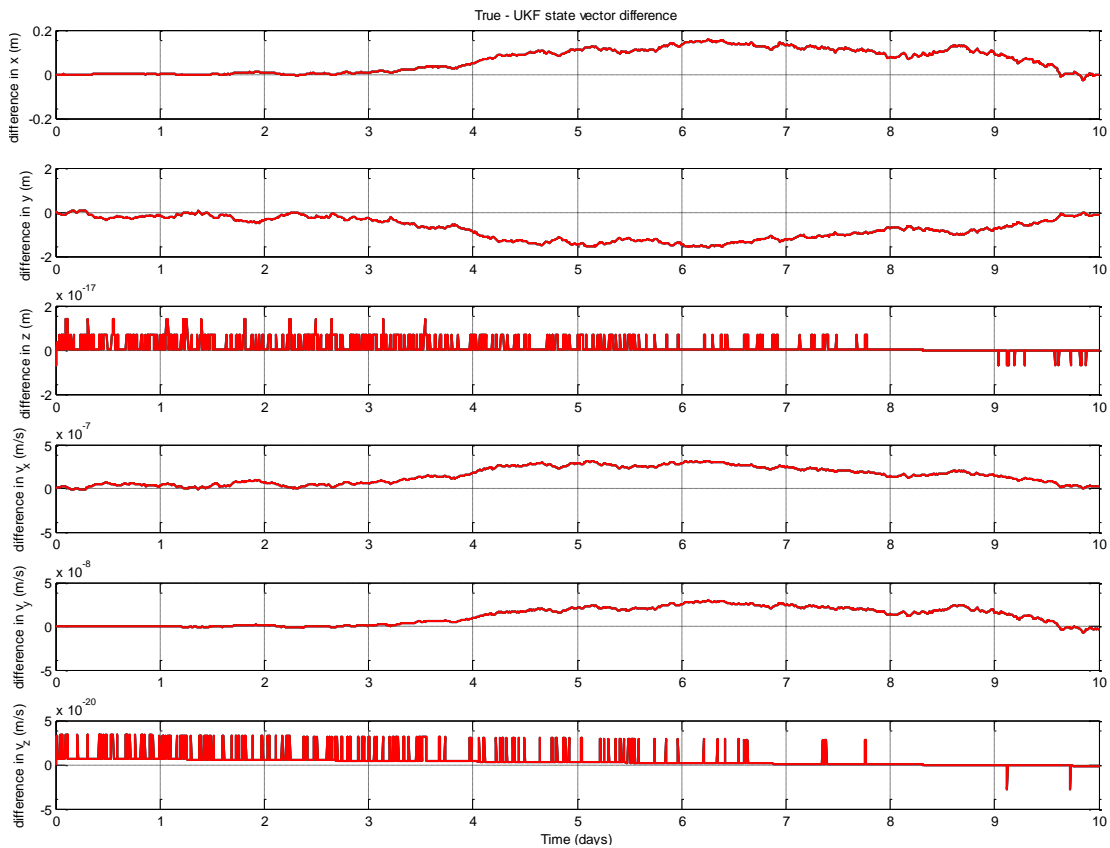


Fig. 5: The difference between the 'true' total orbital state vector and that generated by the UKF. (Y-axis: difference in true total state vector and UKF total state vector ; X-axis: time in days)

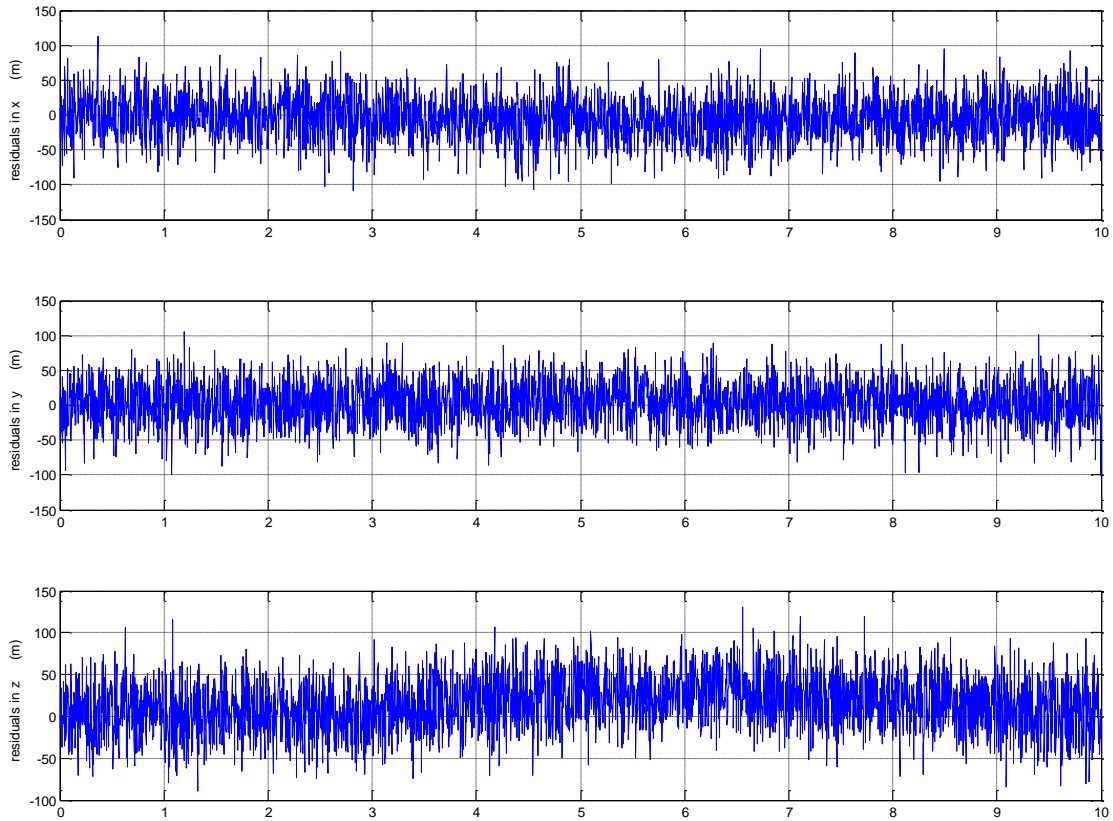


Fig. 6: The measurement residual plot for the position state vector. (Y –axis: difference in true positional state vector and UKF positional state vector ; X – axis: time in days)

CONCLUSION

The results of the simulations prove the principle of navigating using radio-pulsars is indeed possible. The required antenna size, and the processing power and time involved however would currently restrict the use to slow moving earth-based systems.

For the front-end, one immediate conclusion is that a large bandwidth is required in order to reduce the physical size of the system, and that a hybrid solution, employing both incoherent and coherent de-dispersion would be the optimal solution in terms of processing power, as the channel width of a coherent de-dispersion system is still limited by the pulse period and dispersion measure of the particular pulsar in question. In order to allow for real-time processing of the signals for the front-end, all functions would best be transformed into the time domain. This proved quite successful for high SNR situations, and the amount of processing time saved is significant.

The back end performed as advertised, even under extremely noisy scenarios, and the unscented Kalman filter is therefore recommended.

Currently, efforts are being taken to reduce the antenna size and processing power requirements, and perhaps one day allow for the system to be used in space.

WORKS CITED

1. **Lorimer, D. and Kramer, M.** *Handbook of Pulsar Astronomy*. s.l.: Cambridge University Press, 2005.
2. **Hankins, T.H. and Rickett, B.J.** *Pulsar Signal Processing, Methods in Computational Physics, Vol. 14, Radio Astronomy*. 1975. ISBN 0-12-460814-0.
3. **Sheikh, S.** The Use of Variable Celestial X-ray Sources for Spacecraft. *PhD Thesis*. s.l.: University of Maryland, 2005.
4. **Montenbruck, O. and Gill, E.** *Satellite Orbits*. s.l.: Springer, 2000.
5. **Haensel, P.** *Neutron Star 1 'Equation of State and Structure'*. s.l.: Astrophysics and Space Science Library, 2007.
6. **Lorimer, D R, et al.** Multifrequency Flux density measurements of 280 pulsars. *MNRAS*. 1995, 273, pp. 411-421.